Int. J. Solids Structures Vol. 29, No. 18, pp. 2301–2317, 1992
Printed in Great Britain.

0020–7683/92 $5.00 + .00

BOUNDARY ELEMENT ANALYSIS OF CRACKS IN THERMALLY STRESSED PLANAR STRUCTURES

S. T. RAVEENDRA and P. K. BANERJEE
Department of Civil Engineering, State University of New York at Buffalo,
240 Ketter Hall, Buffalo, NY 14260, U.S.A.

(*Received* 10 *October* 1991)

Abstract—The evaluation of stress intensity factors is important for the assessment of structural integrity of flawed structures. The boundary element method is used in the present work for the computation of steady-state and time-dependent stress intensity factors of cracks in thermally loaded structures. While many boundary and volume integral based formulations are available for the treatment of thermoelastic problems in solids, the present analysis is based on a recently developed boundary-only formulation. Crack-tip elements that accurately model the behavior of displacement, temperature fields and singularity of traction, flux fields are used for the accurate evaluation of stress intensity factors.

1. INTRODUCTION

The knowledge of stress intensity factors (SIFs) in thermally stressed structures is very important for the assessment of structural integrity since temperature induced stresses may lead to damage of flawed structural components. The stress intensity factors have been generally obtained analytically for simple structures under steady-state conditions and experimentally and numerically for arbitrary structures under steady-state and time-dependent thermal loading. For example, Emery *et al.* (1977) have used the finite element method (FEM) with singularity programming and quarter point crack elements to compute stress intensity factors for edge cracks. Stress intensity factors for center cracks under a steady-state temperature field were calculated by Sumi and Katayama (1980) using a complex variable method together with analytic continuation and modified mapping-collocation techniques. The stress intensity factors for cracks in planar structures under time-dependent thermal loading have been computed by Hellen *et al.* (1982) using FEM together with quarter point crack elements, J integral and virtual crack extension techniques and by Emmel and Stamm (1985) using FEM with quarter point elements.

The present paper is concerned with the application of a thermoelastic boundary element method for the evaluation of the steady-state and time-dependent stress intensity factors of cracks in finite structures. The BEM has been used extensively for the computation of stress intensity factors since the method is inherently well suited to solve problems of high stress concentration. While the method has been applied previously for the solution of crack problems without body forces, the extension of the method for body force problems is rather limited. For example, stress intensity factors of cracks in rotating solids have been computed recently using a boundary-only integral formulation by Raveendra and Banerjee (1991). As for thermal problems, Tanaka *et al.* (1984) have used an extended boundary integral equation involving a volume integral of the temperature field for the solution of steady- and non-steady-state problems, including fracture mechanics problems. The use of volume discretization for such problems eliminates most of the desirable features of the boundary element method. Further, the displacement and traction variables within each discretized boundary element were not modeled by the higher order interpolation functions that are essential for the accurate computation of stress intensity factors. An alternative boundary integral equation, inappropriately involving displacement and traction rates, was used by Sladek and Sladek (1984) in their thermoelastic analysis. Finally, the boundary integral formulation for steady-state thermoelasticity developed by Rizzo and Shippy (1977) and Cruse *et al.* (1977), based on converting the volume integral involving the temperature field to equivalent surface integrals, was used by Lee and Cho (1990) to compute the thermal

stress intensity factors of cusp cracks. As indicated, the above work is confined to steady-state analysis and only symmetric cracks were considered.

A complete boundary element solution procedure for time-dependent thermoelastic problems, based on integral equations expressed over the surface of the body, was recently developed by Dargush and Banerjee (1989, 1990). In this paper, the method developed by Dargush and Banerjee (1989) for the solution of two-dimensional thermoelastic problems is extended for the solution of thermoelastic fracture mechanics problems. It is well known that when the flow of heat is disturbed by the presence of cracks there develops a discontinuity of heat flux and traction at the crack tips. The accurate evaluation of stress intensity factors depends on how well the temperature and displacement (also flux and traction) fields are approximated in the vicinity of the crack-tips. The strength of singularity in thermoelastic problems is identical to the singularity strength in elastic problems without body forces and therefore, special crack-tip elements that accurately depict the near crack-tip behavior are incorporated into the present analysis. A comparable analysis based on boundary-only integral equations for thermoelasticity together with crack-tip elements that accurately model the temperature, flux and displacement, traction fields near the crack-tip, as used in the present paper, is not currently available in the literature.

2. BEM FORMULATION FOR THERMOELASTICITY

Time-dependent thermoelasticity

The differential equations that govern the quasistatic behavior of a thermoelastic solid, in the absence of internal sources, can be written as

$$c_t \theta_{,ii}(x,t) - \frac{\partial \theta(x,t)}{\partial t} = 0, \quad (\lambda+\mu)u_{i,ij}(x,t) + \mu u_{i,jj}(x,t) - (3\lambda+2\mu)\alpha\theta_{,i} = 0, \quad \text{(1a, b)}$$

where u_i is the displacement vector, θ is the temperature field, λ, μ are Lamé's isothermal elastic constants, α is the coefficient of thermal expansion, c_t is the thermal diffusivity and t is time. For the two-dimensional problem considered in this text, the indices take the values 1, 2. Using the fundamental temperature, displacement solutions due to a unit pulse heat source and a unit point force in an infinite medium and their derivatives, a set of boundary integral equations can be derived (Dargush and Banerjee, 1989):

$$c(\xi)\theta(\xi,t) = \int_S [\bar{g}(x,\xi;t,\tau) * q(x,t) - \bar{f}(x,\xi;t,\tau) * \theta(x,t)]\, \mathrm{d}S(x), \quad \text{(2a)}$$

$$C_{ij}(\xi)u_j(\xi,t) = \int_S [G_{ij}(x,\xi)t_j(x,t) - F_{ij}(x,\xi)u_j(x,t) + g_i(x,\xi;t,\tau) * q(x,t) - f_i(x,\xi;t,\tau) * \theta(x,t)]\, \mathrm{d}S(x), \quad \text{(2b)}$$

where t_i is the traction vector, q is the flux, t is the time at which the responses are calculated, τ is the time at which the pulse source is applied and C_{ij}, c are functions of the local geometry at ξ. The fundamental solutions are:

$G_{ij}(x,\xi)$ and $F_{ij}(x,\xi)$ are the displacement and traction solutions due to a unit point force,
$g_i(x,\xi;t,\tau)$ and $f_i(x,\xi;t,\tau)$ are the displacement and traction solutions due to a unit pulse heat source, and
$\bar{g}(x,\xi;t,\tau)$ and $\bar{f}(x,\xi;t,\tau)$ are the temperature and flux solutions due to a unit pulse heat source.

The fundamental solutions, taken from Dargush and Banerjee (1989), are explicitly given in the Appendix. Note that in the above equations, * denotes a Riemann convolution integral, defined by

$$a * b = \int_0^t a(t,\tau)b(\tau)\,\mathrm{d}\tau. \tag{3}$$

The solution of thermoelastic problems can be obtained by solving the integral equations (2a, b). Since both the space and time variables are involved in the equations, discretization must be introduced in both space and time. Spatially, the variables within each discretized element are assumed to vary quadratically in terms of the values at the nodes of the element and these variables are assumed to be constant during each equally divided time step. Assuming that the time duration is divided into N equal increments of magnitude Δt, the convolution integrals are converted into a series of N terms. That is, the integral equations become

$$c(\xi)\theta(\xi,t) = \sum_{n=1}^{N} \int_S [\delta\bar{g}(x,\xi;t)q(x,t) - \delta\bar{f}(x,\xi;t)\theta(x,t)]\,\mathrm{d}S(x), \tag{4a}$$

$$C_{ij}(\xi)u_j(\xi,t) = \int_S [G_{ij}(x,\xi)t_j(x,t) - F_{ij}(x,\xi)u_j(x,t)]\,\mathrm{d}S(x) + \sum_{n=1}^{N} \int_S [\delta g_i(x,\xi;t)q(x,t) - \delta f_i(x,\xi;t)\theta(x,t)]\,\mathrm{d}s(x), \tag{4b}$$

where

$$\delta g(x,\xi;t) = \int_{(n-1)\Delta t}^{n\Delta t} g(x,\xi;t,\tau)\,\mathrm{d}\tau, \text{ etc.}$$

Since the fundamental solutions are explicitly known the temporal integration can be performed analytically. On the other hand, the spatial integration over discretized elements requires numerical procedures. By considering the singularity of various fundamental solutions these integrals are evaluated using a self-adaptive integration algorithm (Banerjee *et al.*, 1986).

The boundary element solutions require the usual collocation procedure. That is, by evaluating the integral equations at all boundary nodes, we arrive at a set of equations of the form

$$\sum_{n=1}^{N} ([\Delta\bar{g}^{N+1-n}]\{q^n\} - [\Delta\bar{f}^{N+1-n}]\{\theta^n\}) = \{0\}, \tag{5a}$$

$$[\Delta G]\{t^n\} - [\Delta F]\{u^n\} + \sum_{n=1}^{N} ([\Delta g^{N+1-n}]\{q^n\} - [\Delta f^{N+1-n}]\{\theta^n\}) = \{0\}, \tag{5b}$$

where $[\Delta G]$, $[\Delta F]$, $[\Delta g]$, $[\Delta f]$, $[\Delta\bar{g}]$ and $[\Delta\bar{f}]$ are matrices of integrated kernel functions, $\{u\}$, $\{t\}$, $\{\theta\}$, $\{q\}$ are vectors of nodal quantities (i.e. displacement, traction, temperature, flux) and the superscript refers to the time step index. Equation (5a) can be further rearranged by separating the nodal variables for the time step N as

$$[\Delta\bar{g}^1]\{q^N\} - [\Delta\bar{f}^1]\{\theta^N\} = -\sum_{n=1}^{N-1} ([\Delta\bar{g}^{N+1-n}]\{q^n\} - [\Delta\bar{f}^{N+1-n}]\{\theta^n\}). \tag{5c}$$

By imposing the given boundary condition, eqns (5b, c) can be written in terms of the unknown $\{x\}$, $\{X\}$ and the known $\{y\}$, $\{Y\}$ nodal values and associated matrix coefficients as

$$[a^1]\{x^N\} = [b^1]\{y^N\} - \sum_{n=1}^{N-1} ([\Delta\bar{g}^{N+1-n}]\{q^n\} - [\Delta\bar{f}^{N+1-n}]\{\theta^n\}), \tag{6a}$$

$$[A]\{X^N\} = [B]\{Y^N\} - \sum_{n=1}^{N} ([\Delta g^{N+1-n}]\{q^n\} - [\Delta f^{N+1-n}]\{\theta^n\}). \tag{6b}$$

Note that the matrices $[A]$, $[B]$ are made up of time-independent kernel coefficients and matrices $[a^1]$, $[b^1]$ are obtained from the kernels of the first time step and therefore, these matrices need to be formed only once during the solution process. The decomposition of matrices $[A]$ and $[a^1]$, obtained from the solution at the first time step, is then used for the solution of nodal values at subsequent time steps for different right-hand sides. The right-hand side is made up of known boundary conditions and the accumulated effect of temperature and flux history up to the current time step, which are known at a given time step.

Steady-state thermoelasticity

The thermoelastic boundary element formulation simplifies considerably under steady-state conditions. The governing differential equations now become

$$k\theta_{,ii}(x) = 0, \qquad (\lambda+\mu)u_{j,ij}(x) + \mu u_{i,jj}(x) - (3\lambda+2\mu)\alpha\theta_{,i}(x) = 0, \tag{7a, b}$$

where k is the thermal conductivity. Using the fundamental temperature and displacement solutions due to time-independent unit load and unit step heat source a set of integral equations can be derived (Dargush and Banerjee, 1989):

$$c(\xi)\theta(\xi) = \int_S [\bar{q}(x,\xi)q(x) - \bar{f}(x,\xi)\theta(x)]\,dS(x), \tag{8a}$$

$$C_{ij}(\xi)u_j(\xi) = \int_S [G_{ij}(x,\xi)t_j(x) - F_{ij}(x,\xi)u_j(x)]\,dS(x) + \int_S [g_i(x,\xi)q(x) - f_i(x,\xi)\theta(x)]\,dS(x). \tag{8b}$$

Since only spatial variables are involved the solution requires only the discretization of the boundary of the problem domain. A set of algebraic equations for each set of integral equation can be obtained through the collocation process and the unknown nodal values are computed by imposing the boundary condition. The final set of equations can be expressed as

$$[a]\{x\} = [b]\{y\}, \qquad [A]\{X\} = [B]\{Y\} - ([\Delta g]\{q\} - [\Delta f]\{\theta\}). \tag{9a, b}$$

3. FRACTURE MECHANICS MODELING OF THERMAL PROBLEMS

In the presence of cracks the integral equations, described in the previous section, cannot be applied directly. Unless the problem geometry and loading are symmetrical with respect to the crack plane the BEM procedure requires the modeling of co-planar surfaces of the crack. Since identical equations are obtained at corresponding nodes of the crack surfaces, the resulting system matrix becomes ill-conditioned. A simple, but elegant, procedure which is effective for the solution of non-symmetric crack problems is the multi-region approach. In this approach, the body is divided into sub-regions along the crack plane and the integral equations are applied independently for each region. The final solution is obtained by coupling the equations of both regions through compatibility and continuity conditions.

Thermoelastic problems, in the absence of cracks, can be solved accurately by interpolating the field variables within each discretized element by quadratic shape functions. It is well known that the disturbance of heat flow by crack surfaces will produce singularity of temperature and displacement derivative fields. Therefore, the accuracy of the solution

depends considerably on how well the temperature, displacement and flux, traction fields are approximated in the vicinity of the crack tip. The usually quadratic boundary elements provide neither the correct $\sqrt{\rho}$ variation of the crack-tip displacement and temperature fields nor the required singularity of the traction and flux fields. The correct variation of displacement and temperature fields can be obtained through the use of quarter point elements (Barsoum, 1976). That is, by placing the mid-nodes of sides emanating from the crack at geometric quarter points, the variation of displacement and temperature fields is forced to an asymptotic $\sqrt{\rho}$ behavior as

$$\{u(\rho)\} = A_1 + A_2\sqrt{\frac{\rho}{l}} + A_3\frac{\rho}{l}, \tag{10}$$

where A_i are functions of nodal values and l is the element length. Unlike the finite element method, the derivatives of displacements and temperatures are independently approximated in the BEM and therefore the use of the quarter point elements will provide the incorrect variation of traction and flux. The correct singularity of traction and flux fields can be secured by multiplying the nominal traction and flux fields, obtained from the quarter point modeling, by a non-dimensional parameter $\sqrt{(l/\rho)}$ such that

$$\{t(\rho)\} = \sqrt{\frac{l}{\rho}}\{\hat{t}(\rho)\} = B_1\sqrt{\frac{l}{\rho}} + B_2 + B_3\sqrt{\frac{\rho}{l}}, \tag{11}$$

where B_i are functions of nodal values and $\hat{t}_i$ is the vector of nominal traction (flux) obtained from quarter point element modeling.

Evaluation of stress intensity factors

Thermal stresses can be determined from the theory of elasticity equations with body forces obtained from solving the pure temperature problem. Therefore, the distribution of stresses (and strains) near the crack tip in a thermoelastic problem is given by the general equations that are applicable in linear elastic fracture mechanics. That is, the near crack tip stress field σ_{ij}, due to remote loading, may be expressed in terms of the distance from the crack tip ρ (Fig. 1):

$$\sigma_{ij} = \frac{a_{ij}^0}{\sqrt{\rho}} + a_{ij}^1 + a_{ij}^2\sqrt{\rho} + \cdots \tag{12}$$

This crack-tip stress field may also be expressed in terms of a singularity strength parameter known as a stress intensity factor. These stress intensity factors are defined as (Kanninen and Popelar, 1985):

$$\begin{Bmatrix} K_{\mathrm{I}} \\ K_{\mathrm{II}} \end{Bmatrix} = \lim_{\rho \to 0} \sqrt{2\pi\rho} \begin{Bmatrix} \sigma_{22}|_{\theta=0} \\ \sigma_{12}|_{\theta=0} \end{Bmatrix}, \tag{13}$$

where K_{I} and K_{II} are the mode I and mode II stress intensity factors, respectively. Using the definition of stress intensity factors and eqn (11), the stress intensity factors may be calculated from nominal tractions at the crack tip as

$$\begin{Bmatrix} K_{\mathrm{I}} \\ K_{\mathrm{II}} \end{Bmatrix} = \sqrt{2\pi l} \begin{Bmatrix} \hat{t}_2^0 \\ \hat{t}_1^0 \end{Bmatrix}, \tag{14}$$

where $\hat{t}_i^0$ is the nominal traction at the crack tip. It should be noted that although the tractions t_i^0, at the crack tip are unbounded, the nominal tractions are finite.

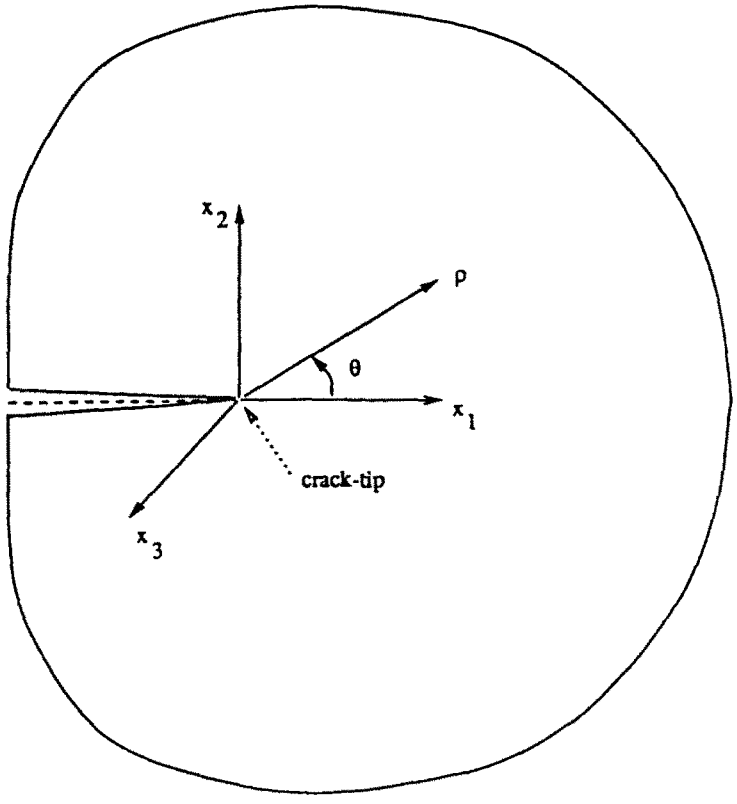

Fig. 1. Definition of crack geometry.

Alternatively, the stress intensity factors may be expressed in terms of crack opening displacements $\Delta u_i = u_i|_{\theta=\pi} - u_i|_{\theta=-\pi}$ (Kanninen and Popelar, 1985):

$$\begin{Bmatrix} K_I \\ K_{II} \end{Bmatrix} = \frac{H}{8}\sqrt{\frac{2\pi}{\rho}} \begin{Bmatrix} \Delta u_2 \\ \Delta u_1 \end{Bmatrix}, \tag{15}$$

where, in terms of Young's modulus E and Poisson's ratio ν, $H = E$ for the plane stress case and $H = E/(1-\nu^2)$ for the plane strain case.

From past experience, it was found that the crack-tip nominal traction depends very much on the accuracy of the numerical integration scheme employed for the evaluation of higher order singular integrals (Raveendra and Banerjee, 1991). Since the crack-tip displacements are less sensitive to the integration scheme used, the stress intensity factors in the present analysis are computed from the crack-opening displacements.

4. NUMERICAL EXAMPLES

Effect of crack-tip elements

To assess the accuracy of the solution procedure described in this text, the mode I stress intensity factors for an edge crack, shown in Fig. 2, were computed under steady-state thermal conditions. The applied temperature field was

$$T = T_0(-1+2x/b).$$

The normalized stress intensity factor for this situation is obtained analytically by Hellen *et al.* (1982) using Green's integral:

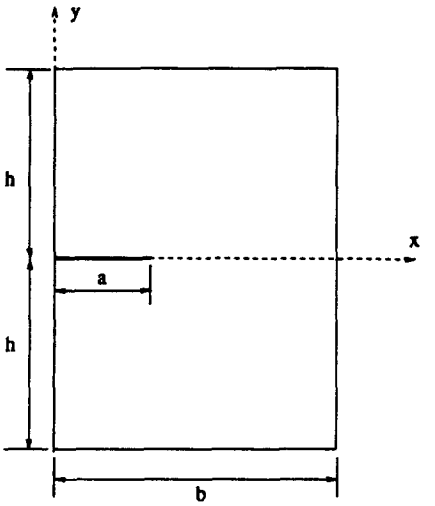

Fig. 2. Geometry of an edge crack in a rectangular plane.

$$\frac{K_I}{K_0} = \frac{4.48}{\sqrt{\pi}} \sqrt{\frac{a}{b}} \left[\frac{\pi}{4} - \frac{a}{b} \right],$$

where $K_0 = E\alpha T_0 \sqrt{b}$ for plane stress and $K_0 = E\alpha T_0 \sqrt{b}/(1-\nu)$ for plane strain. The stress intensity factor was calculated using regular quadratic elements in one case and quarter point elements with traction singular modification at crack tips in another case. The crack geometry used was $a/b = 0.1$ and $h/b = 2$. The stress intensity factors obtained from regular quadratic boundary elements deviated from the analytical solution by about 7%, but the analytical and boundary element results were within 1% when quarter point elements with traction singular modification were used at the crack tip. This confirms the need to use special elements at the crack tip and, therefore, these elements were used in all the subsequent analyses.

It should be noted that one half of the crack was modeled by three elements in both cases. It is possible to improve the accuracy of the results of the first case by using finer discretization, which increases the computing effort. However, highly accurate results can be obtained through the use of special crack-tip elements even with a relatively coarse mesh.

Steady-state thermal analysis of a center crack

The steady-state stress intensity factors of a center crack in a finite rectangular plate, shown in Fig. 3, were computed using BEM under plane strain conditions. This problem was solved previously using the complex variable method together with the modified collocation technique by Sumi and Katayama (1980) and also by Emmel and Stamm (1985) using the quarter point finite element method. The thermal boundary conditions used were

$$T = T_1 \text{ (constant)}, \quad |x| \leqslant a, y = 0\pm; \quad T = T_2 \text{ (constant)}, \quad |x| = b, |y| < h;$$
$$T = T_2 \text{ (constant)}, \quad |y| = h, |x| < b,$$

for case A, and for case B,

$$\frac{\partial T}{\partial y} = 0, \quad |x| \leqslant a, y = 0\pm; \quad \frac{\partial T}{\partial x} = 0, \quad |x| = b, |y| < h;$$
$$T = \pm T_2 \text{ (constant)}, \quad |x| < b, y = \pm h.$$

The mode I stress intensity factors computed from case A were normalized with respect to $K_0 = \alpha E(T_2 - T_1)\sqrt{b}/(1-\nu)$, and the mode II stress intensity factors computed from

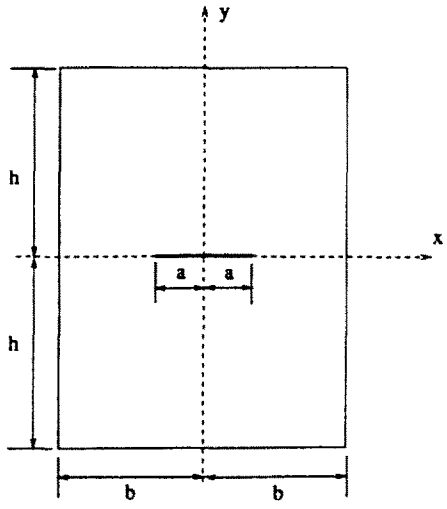

Fig. 3. Geometry of a center crack in a rectangular plate.

case B were normalized with respect to $K_0 = \alpha E T_2 \sqrt{b}/(1-\nu)$. The results, shown in Fig. 4, indicate excellent agreement between the present BEM solutions and results given in the cited references.

Steady-state thermal analysis of an edge crack

The next steady-state example considered is the problem of an edge crack in a finite rectangular plate, shown in Fig. 2, solved previously using various finite element techniques by Hellen *et al.* (1982). The thermal boundary condition used were

$$T = T_0(-1+2x/b); \quad \frac{\partial T}{\partial y} = 0, \quad |y| = h, \quad 0 < x < b; \quad \frac{\partial T}{\partial y} = 0, \quad y = 0, \quad x \leqslant a.$$

The non-dimensional form of the stress intensity factors were obtained by dividing the

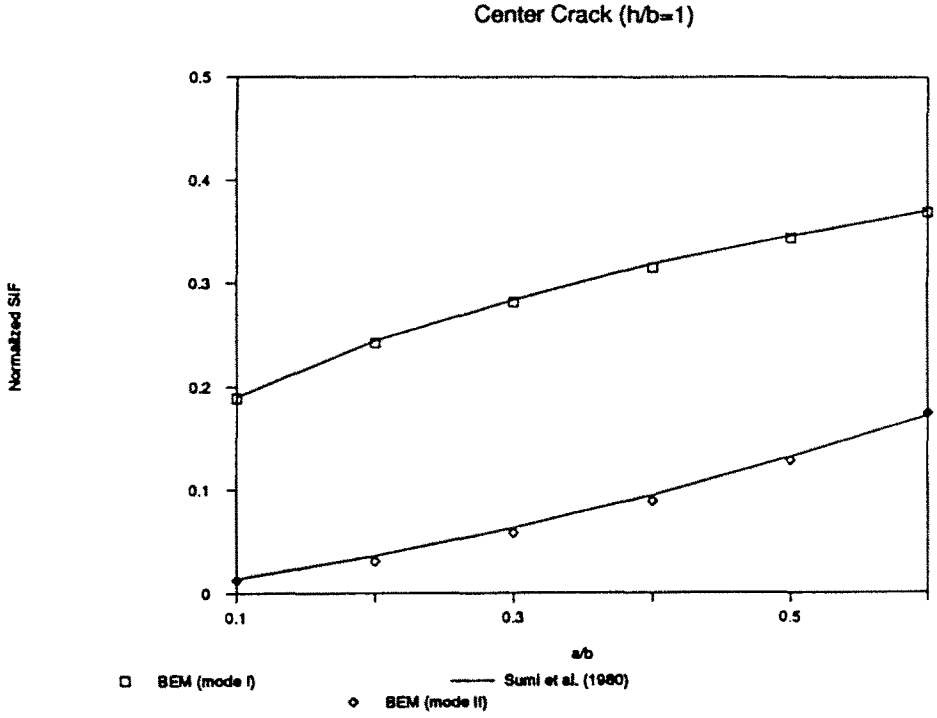

Fig. 4. Comparison of Mode I and II steady-state SIFs for a center crack.

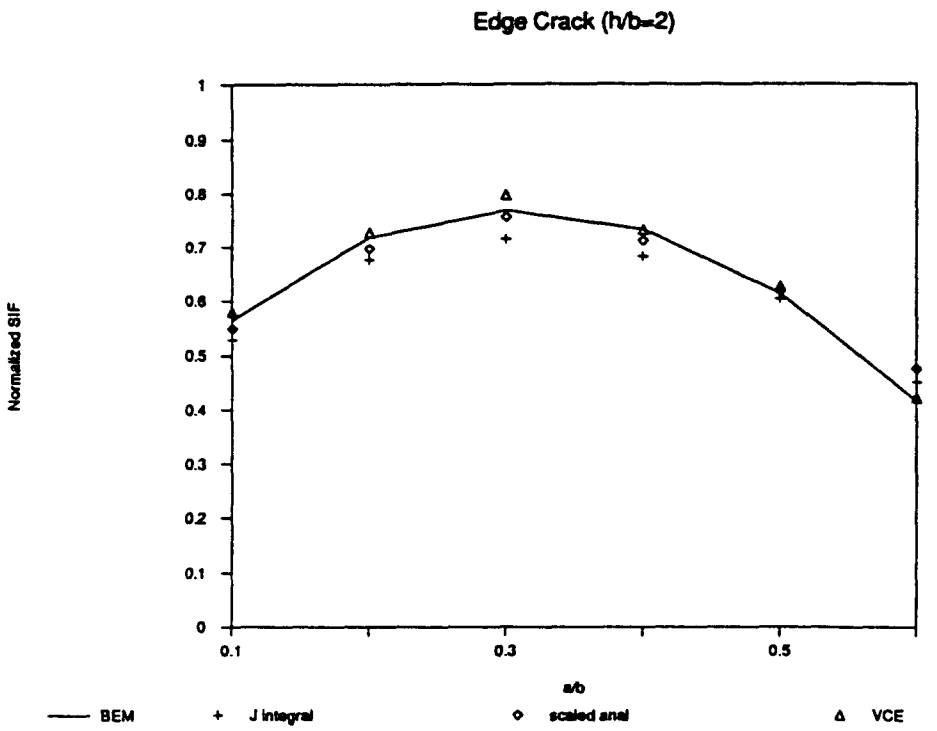

Fig. 5. Comparison of Mode I steady-state SIFS for an edge crack.

plane stress solutions by $K_0 = E\alpha T_0\sqrt{b}$. The finite element results were computed using the virtual crack extension (VCE) technique, J integral technique and from a semi-analytical solution based on Green's integral which was scaled by a factor that depends on the geometry a/b of the plate. The finite element results are compared to BEM solutions in Fig. 5. Again the figure shows good agreement between the solutions.

Steady-state thermal analysis of radial crack

The final steady-state example considered is the problem of a radial crack in a hollow cylinder. The geometry of the cylinder is shown in Fig. 6. The crack geometry used was $a = 4.0$, $a/b = 0.2$ and $R_i/R_0 = 0.8$. The steady-state stress intensity factors were computed under three sets of thermal boundary conditions. The boundary conditions used were:

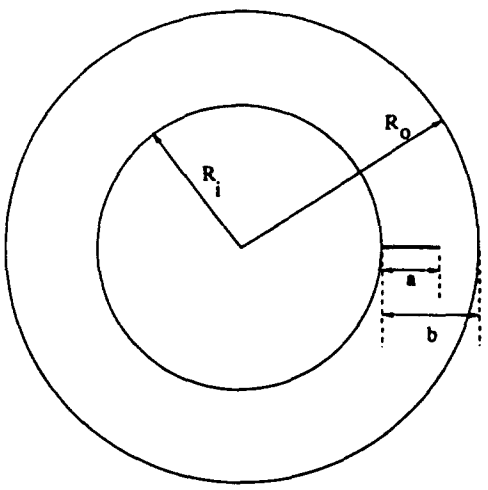

Fig. 6. Geometry of a radial crack in a hollow cylinder.

Case A: A thermal loading of $-T^0$ was applied to the inner surface of the cylinder and to the crack surface and the outer surface of the cylinder was maintained at 0°.
Case B: The inner surface of the cylinder was cooled to a temperature of $-T^0$ while the outer surface was maintained at 0°. The crack surfaces were assumed to be insulated.
Case C: The outer surface of the cylinder was heated to a temperature of T^0 while the inner surface of the cylinder and the crack surfaces were kept at 0°.

Figure 7 shows that the normalized stress intensity factors were essentially identical for all three cases and the SIFs increase monotonically with the non-dimensional crack length parameter. The stress intensity factors were normalized by dividing the boundary element solutions by $K_0 = E\alpha\Delta T\sqrt{b}/(1-\nu)$, where ΔT is the difference in temperatures between the inner and outer surfaces.

Time-dependent thermal analysis of center cracks

A limited number of fracture mechanics analysis problems with transient temperature distribution is available in the literature. One such example is the evaluation of the transient stress intensity factor of a center crack in a rectangular plate using the finite element method (Emmel and Stamm, 1985). The thermal loading considered in the present analysis corresponds to $T = T_2$ on the boundary and $T = 0$ on the crack surface. The finite element mode I SIF results, for a crack geometry of $a/h = 0.5$, $h/b = 1$ (see Fig. 3), are given in Emmel and Stamm (1985). A comparison of FEM results with the corresponding solutions of BEM is shown in Fig. 8. The results show that the two numerical solutions are in good agreement. Further, BEM solutions for crack geometry $a/h = 0.1$ and $a/h = 0.3$ are also shown in the figure. All the results indicate that the normalized stress intensity factors increase monotonically to their steady-state values. It should be noted that the time axis is non-dimensionalized as $c_p t/b^2$, where c_p is the thermal diffusivity, t is time and b is the plate width. The value used for diffusivity in the finite element solutions is not given in the reference, therefore, a value for c_p was assumed such that the time values were shifted to the corresponding BEM values. Note that the values of SIFs shown for the final time step in this plot and all the subsequent plots are obtained from the steady-state analysis.

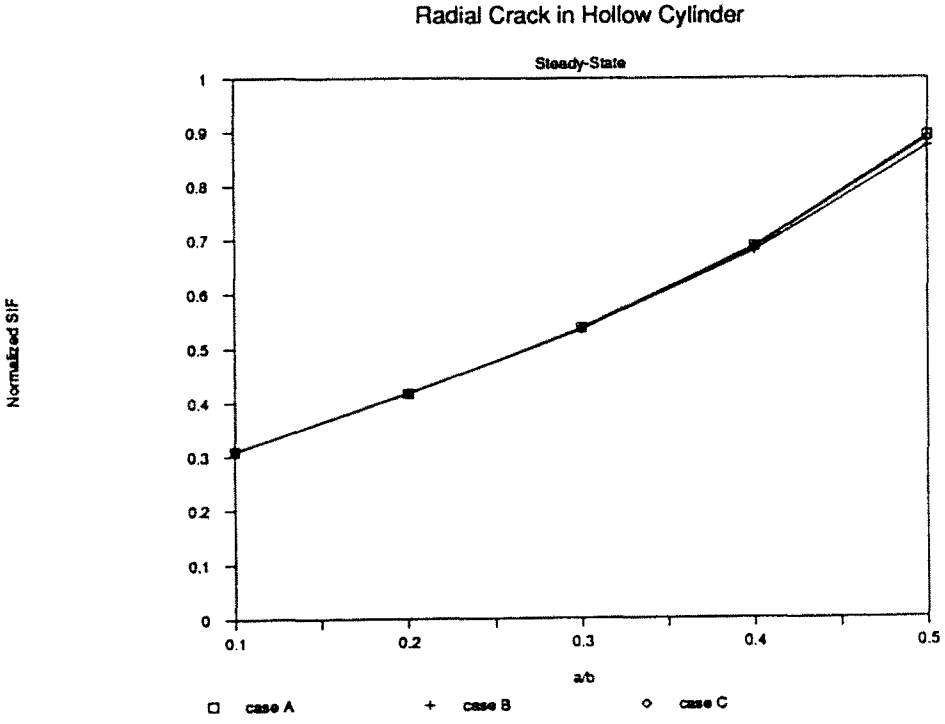

Fig. 7. Steady-state SIFs for a radial crack.

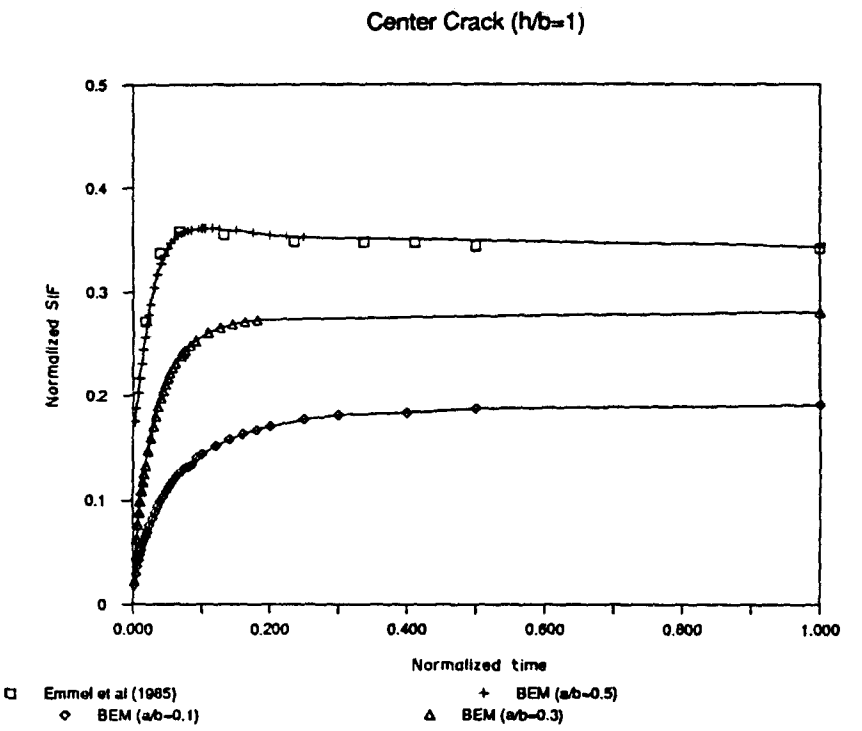

Fig. 8. Comparison of transient SIFs for a center crack.

Time-dependent thermal analysis of edge cracks

The transient stress intensity factors for an edge crack (Fig. 2) were calculated by Hellen *et al.* (1982) using the finite element method. Only one geometry ($a/b = 0.3$) was considered in the finite element study. The plate was constrained along the vertical direction at the top and bottom faces and the left side of the plate was cooled to $-2T^{\circ}$, while the opposite side was kept at 0°. The FEM results are given for a crack geometry of $a/b = 0.3$. The BEM solutions, shown in Fig. 9, agree well with the finite element results. In this case also, the stress intensity factor and time values were non-dimensionalized as in the previous example. Additionally, boundary element results were obtained for crack geometries of $a/b = 0.1$ and $a/b = 0.5$. These results also increase rapidly to their steady-state values.

Time-dependent thermal analysis of a radial crack in a hollow cylinder

This example, for a specific geometry of $a/b = 0.2$, was also examined by Hellen *et al.* (1982) and Emmel and Stamm (1985) using the finite element method. Three thermal loading cases, described previously in the steady-state example, were also considered in the present problem. Figure 10 shows a comparison of boundary element solutions to finite element results for the thermal loading given by case A. The stress intensity factors were normalized as in the steady-state example and the time values were non-dimensionalized as $c_1 t/b^2$. The figure shows that the FEM results and BEM solutions are in good agreement. The BEM solutions are also compared to the FEM results for cases B and C in Figs 11 and 12, respectively. Again the FEM and BEM results are in good agreement.

Time-dependent thermal analysis of an inclined crack in a rectangular plate

Finally, a mixed mode crack problem under transient thermal loading was considered. A crack inclined at an angle of 22.5° to the horizontal, embedded in a rectangular plate, was selected. The crack geometry used was $a/b = 0.2$, $h/b = 1$, as shown in Fig. 13. A

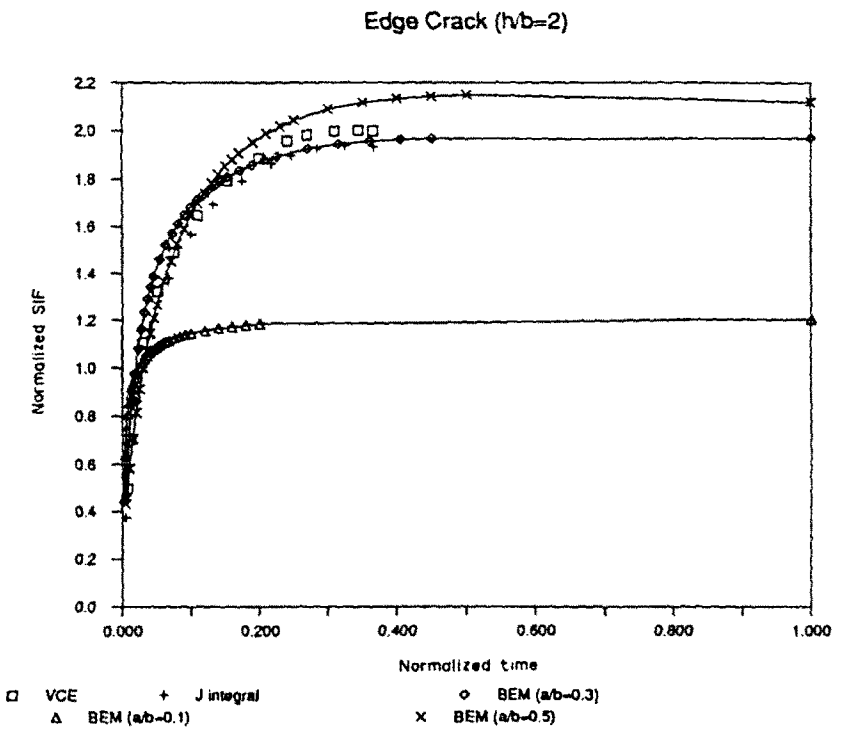

Fig. 9. Comparison of transient SIFs for an edge crack.

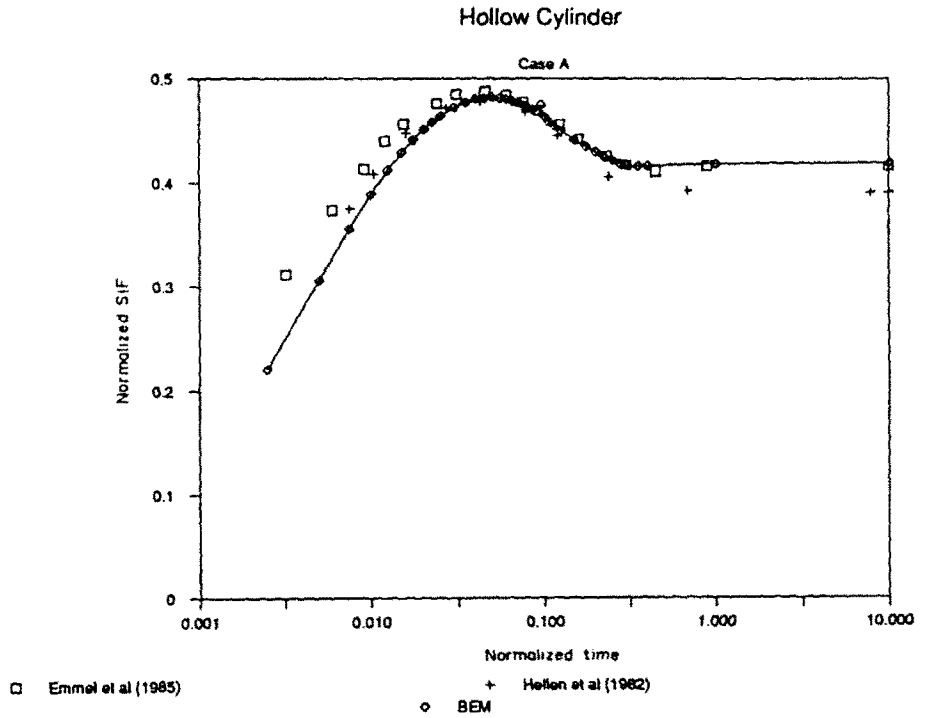

Fig. 10. Comparison of transient SIFs for a radial crack (case A).

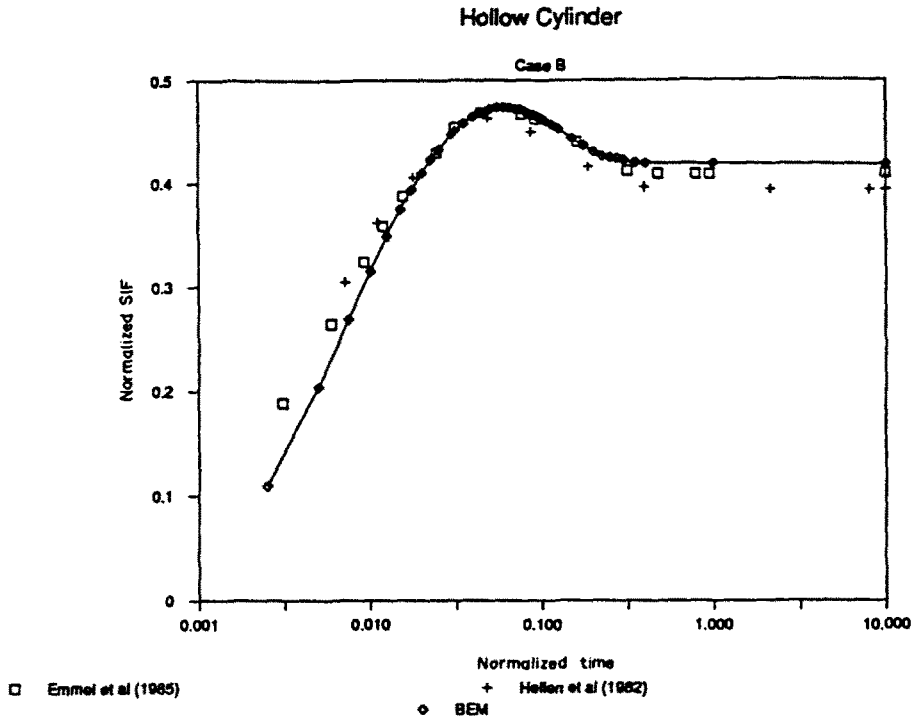

Fig. 11. Comparison of transient SIFs for a radial crack (case B).

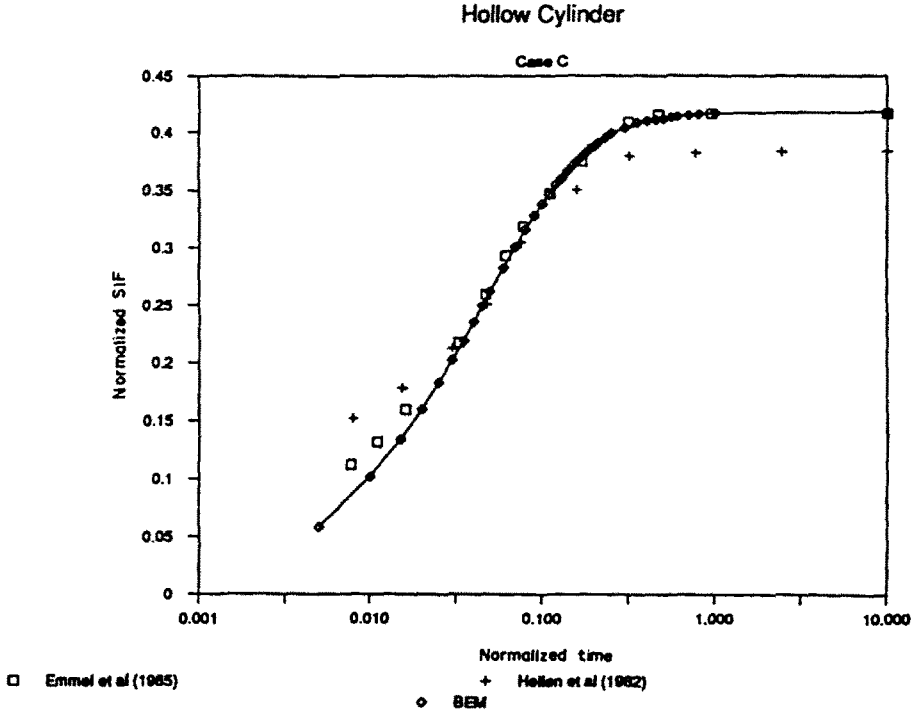

Fig. 12. Comparison of transient SIFs for a radial crack (case C).

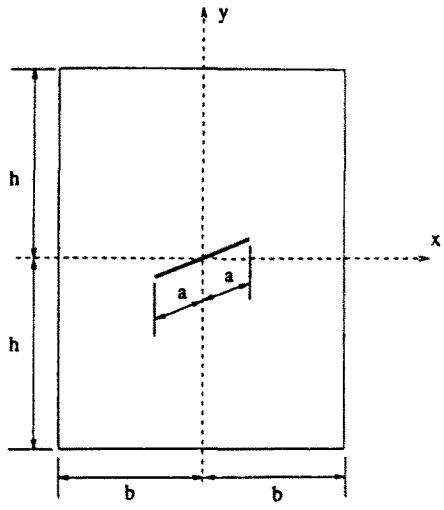

Fig. 13. Geometry of an inclined crack in a rectangular plate.

thermal loading of 0° at the crack surface and T° at the outer boundary, applied at time $t = 0$ and maintained at those values, was considered. The variation of mode I and mode II stress intensity factors with time is shown in Figs 14 and 15, respectively. The stress intensity factors and times were non-dimensionalized as in the center crack example. Figure 14 indicates that the mode I stress intensity factor increases monotonically to the steady-state value, however, the mode II stress intensity factor increases to a peak after a short time before it decreases gradually to the steady-state value, as shown in Fig. 15.

Some aspects of modeling

The magnitude of the time step used in solving the examples in the present work is not indicated since the results are not very sensitive to the time step size. Dargush and Banerjee

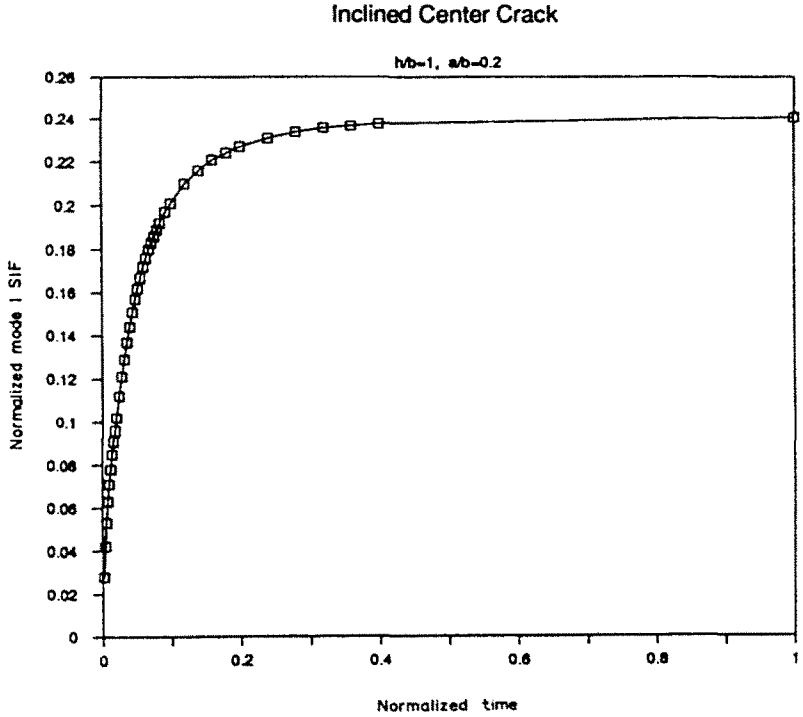

Fig. 14. Transient mode I SIFs for an inclined crack.

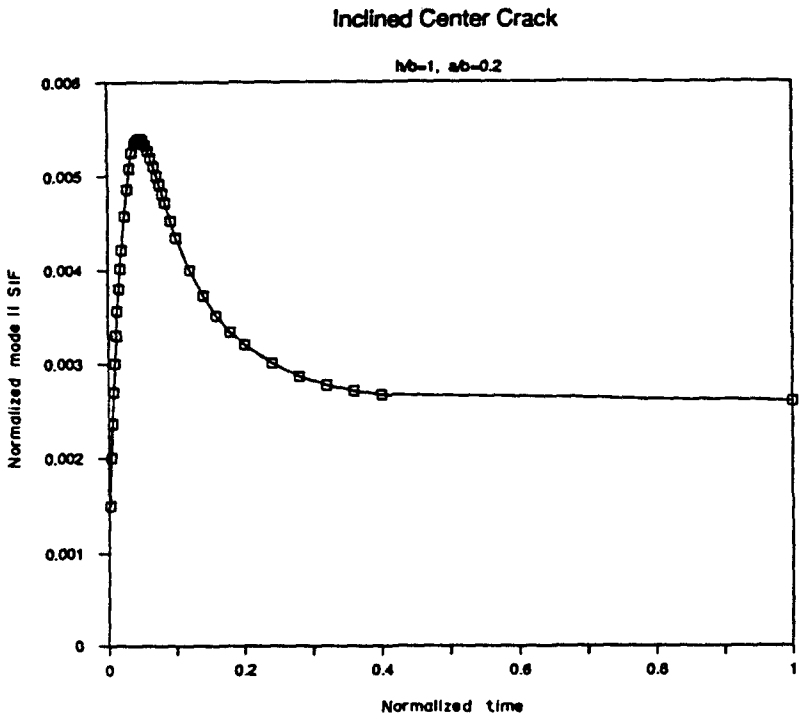

Fig. 15. Transient mode II SIFs for an inclined crack.

(1989), in their transient thermoelastic analysis, have estimated the optimum time step from thermal diffusivity c_p, and the size of the smallest element L, as $\delta t = 0.05L^2/c_p$. In the present work, instead of the element size, the half-length of the crack was used in estimating the time step. However, the results are insensitive even to the use of time steps that are several time bigger than the estimated values. This is consistent with a recent observation of Dargush and Banerjee (1991) in the analysis of transient heat conduction. Generally, the size of time step only seems to affect the very early responses.

In general, half the crack length was modeled by three boundary elements. The same discretization was used on both sides of the crack tip. Quarter point crack-tip elements with traction singular modification were used at the crack tip. The element sizes, thereafter, were increased gradually. This discretization pattern was developed during the course of previous fracture mechanics analyses [e.g. Raveendra and Banerjee (1991)].

5. CONCLUSION

A knowledge of stress intensity factors is important in the evaluation of the structural integrity of flawed structures. A boundary-only integral equation is applied for the first time for the evaluation of stress intensity factors of planar structures subjected to steady-state and transient thermal loading. Since the accuracy of the solution depends considerably on the correct representation of near-tip fields, special crack-tip elements are used at the crack-tip. These elements provide the correct variation of displacement, temperature fields and singularity of traction, flux fields. Center cracks, edge cracks and an inclined crack in a plate and a radial crack in a cylinder are solved using this boundary element procedure. Most of the BEM solutions are compared to previous results obtained from finite element and analytical methods to validate the applicability of the BEM procedure. The efficient and accurate boundary element method used in the present analysis provides an elegant alternative to other numerical methods for the solution of steady-state and transient thermal fracture mechanics problems.

REFERENCES

Banerjee, P. K., Ahmad, S. and Manolis, G. D. (1986). Transient elastodynamic analysis of three-dimensional problems by boundary element method. *Earthquake Engng Struct. Dynamics* **14**, 933–949.

Barsoum, R. S. (1976). On the use of isoparametric finite elements in linear fracture mechanics. *Int. J. Numer. Meth. Engng* **10**, 25–37.

Cruse, T. A., Snow, D. W. and Wilson, R. B. (1977). Numerical solution in axisymmetric elasticity. *Comput. Struct.* **7**, 445–451.

Dargush, G. F. and Banerjee, P. K. (1989). Development of a boundary element method for time-dependent planar thermoelasticity. *Int. J. Solids Structures* **25**(9), 999–1021.

Dargush, G. F. and Banerjee, P. K. (1990). Boundary element methods in three-dimensional thermoelasticity. *Int. J. Solids Structures* **26**(2), 199–216.

Dargush, G. F. and Banerjee, P. K. (1991). Application of the boundary element method to transient heat conduction. *Int. J. Numer. Engng* **31**, 1231–1247.

Emery, A. F., Neighbors, P. K., Kobayashi, A. S. and Love, W. J. (1977). Stress intensity factors in edge-cracked plates subjected to transient thermal singularities. *J. Pres. Ves. Tech.* **99**, 100–104.

Emmel, E. and Stamm, H. (1985). Calculation of stress intensity factors of thermally loaded cracks using the finite element method. *Int. J. Press. Ves. Piping* **19**, 1–17.

Hellen, T. K., Cesari, F. and Maitan, A. (1982). The application of fracture mechanics in thermally stressed structure. *Int. J. Pres. Ves. Piping* **10**, 181–204.

Kanninen, M. F. and Popelar, C. H. (1985). *Advanced Fracture Mechanics*. Oxford University Press, New York.

Lee, K. Y. and Cho, Y. H. (1990). Boundary element analysis of thermal stress intensity factors for cusp cracks. *Engng Fract. Mech.* **37**(4), 787–798.

Raveendra, S. T. and Banerjee, P. K. (1991). Analysis of rotating solids with cracks by the boundary element method. *Int. J. Solids Structures* **28**(9), 1155–1170.

Rizzo, F. J. and Shippy, D. J. (1977). An advanced boundary integral equation method for three-dimensional thermoelasticity. *Int. J. Numer. Meth. Engng* **11**, 1753–1768.

Sladek, V. and Sladek, J. (1984). Boundary integral equation method in two-dimensional thermoelasticity. *Engng Anal.* **1**, 135–148.

Sumi, N. and Katayama, T. (1980). Thermal stress singularities at tips of a Griffith crack in a finite rectangular plate. *Nucl. Engng Des.* **60**, 389–394.

Tanaka, M., Togoh, H. and Kikuta, M. (1984). Boundary element method applied to 2-D thermoelastic problems in steady and non-steady states. *Engng Anal.* **1**(1), 13–19.

APPENDIX

Time-dependent thermoelasticity

The temperature and displacement fundamental solutions due to a unit pulse heat source are

$$g(x,\xi;t) = c_1 h_1(\eta), \quad g_i(x,\xi;t) = c_2 y_i h_2(\eta). \tag{A1, 2}$$

The displacement fundamental solution due to a unit point load is

$$G_{ij}(x,\xi) = C_1[z_i z_j - \delta_{ij} C_2 \ln r], \tag{A3}$$

where

$$c_1 = 1/2\pi k, \quad c_2 = \beta c_1/2(\lambda+2\mu), \quad C_1 = 1/8\pi\mu(1-\nu), \quad C_2 = 3-4\nu, \quad z_i = y_i/r, \quad r^2 = y_i y_i,$$

$$y_i = x_i - \xi_i, \quad \eta = r/\sqrt{c_1 t}, \quad h_0 = \frac{2}{\eta^2}(1-e^{-\eta^2/4}), \quad h_1 = \tfrac{1}{2}E_1(\eta^2/4), \quad E_1(\eta) = \int_\eta^\infty \frac{e^{-x}}{x}\,dx, \quad h_2 = h_0 + h_1.$$

The flux and traction fundamental solutions are obtained from the appropriate derivatives of temperature and displacement solutions as

$$f(x,\xi;t) = \frac{c_3}{r} z_k n_k h_1(\eta), \quad f_i(x,\xi;t) = c_4[2z_i z_k n_k h_0(\eta) - n_i h_2(\eta)], \tag{A4, 5}$$

$$F_{ij} = \frac{C_3}{r}[2z_i z_j z_k n_k + C_4(\delta_{ij} z_k n_k + z_i n_j)], \tag{A6}$$

where

$$c_3 = kc_1, \quad c_4 = kc_2, \quad C_3 = -2\mu C_1, \quad C_4 = 1-2\nu, \quad h_3 = e^{-\eta^2/4}.$$

Steady-state thermoelasticity

The fundamental solutions G_{ij} and F_{ij} are the same as those given by eqns (A3 and 6). The steady-state solutions $\bar{g}$, $\bar{f}$, g_i and f_i are obtained from the time-dependent solutions as t approaches infinity. That is, the steady-state fundamental solutions are

$$\bar{g}(x,\xi) = -c_1 \ln r, \quad \bar{f}(x,\xi) = \frac{c_3}{r} z_k n_k, \tag{A7, 8}$$

$$g_i(x,\xi) = \frac{c_2}{2}[r_i(1-2\ln r)] \quad \text{and} \quad f_i(x,\xi) = \frac{c_4}{2}[2z_i z_k n_k - n_i(1-2\ln r)]. \tag{A9, 10}$$